

Canted ferromagnetism in $\text{RuSr}_2\text{GdCu}_2\text{O}_8$

Kohji Nakamura^{1,2,*} and A. J. Freeman²

¹*Department of Physics Engineering, Mie University, Tsu, Mie 514-8507, Japan*

²*Department of Physics and Astronomy, Northwestern University, Evanston, IL60208*

(Dated: October 28, 2018)

First principles calculations using the full-potential linearized augmented plane wave (FLAPW) method including intra-atomic noncollinear magnetism have been performed to determine the magnetic structures of $\text{RuSr}_2\text{GdCu}_2\text{O}_8$. The magnetism clearly arises from the RuO_6 octahedra where the moments on neighboring Ru sites order antiferromagnetically but cant perpendicular to the AFM axis - and so induce a weak ferromagnetism. The projected Ru moments along the AFM and FM axes result in magnetic moments of 1.16 and $0.99\mu_B$ respectively. The results are consistent with the possible coexistence of canted ferromagnetism and superconductivity in the $\text{RuSr}_2\text{GdCu}_2\text{O}_8$ - inferred from experiments.

PACS numbers: 75.25.+z 74.25.Jb 74.25.Ha 74.72.Jt

The coexistence of magnetism and superconductivity on a microscopic scale has recently been reported in $\text{RuSr}_2\text{RCu}_2\text{O}_8$ ($\text{R}=\text{Gd}$, Eu and Y).^{1,2,3} These materials have an analogy to the superconductivity in the two-dimensional high T_c cuprate superconductors associated with the Cu e_g states of the CuO_2 layers. The superconductivity appears below a superconducting transition temperature, $T_c = 30\text{-}50$ K. The magnetism arises from the Ru t_{2g} states of the RuO_6 octahedra, which do not produce any significant effects on the superconductivity since the Ru t_{2g} electrons do not couple to the Cu e_g states regardless of the ordering of the magnetic Ru moments.^{4,5}

Although the Ru moments order magnetically below a magnetic transition temperature, $T_m = 130\text{-}150$ K, the type of ordering still remains controversial. An earlier report of a homogeneous ferromagnetic (FM) ordering of the Ru moments by dc magnetization and muon spin rotation experiments¹ has been brought into a question by neutron diffraction experiments,⁶ suggesting an antiferromagnetic (AFM) G-type ordering where nearest neighbors of the Ru moments along all three crystallographic axes are coupled antiferromagnetically. First-principles calculations also demonstrated that the AFM ordering is energetically favored over the FM one within the collinear magnetic structures.⁵ Nevertheless, recent magnetization and magnetic resonance experiments^{7,8,9} have provided clear evidence of a weak ferromagnetism. To account for complexity in the magnetism, noncollinear magnetism such as canting of the Ru moments has been proposed,^{2,10} to induce a ferromagnetic component.

Here, we determine from first-principles the magnetic structures in $\text{RuSr}_2\text{GdCu}_2\text{O}_8$ by using the highly precise full-potential linearized augmented plane-wave (FLAPW) method¹¹ that includes intra-atomic noncollinear magnetism which can describe the canting of the Ru moments. Indeed, we find that the moments on neighboring Ru sites order antiferromagnetically but cant perpendicular to the AFM axis - and so induce a weak ferromagnetism.

In the calculations, we employed a crystal structure

with the $P4/mbm$ space group determined by neutron diffraction experiments.¹² This structure is similar to that of $\text{YBa}_2\text{Cu}_3\text{O}_7$, where Y, Ba and Cu (chain atoms) are replaced by Gd, Sr and Ru, respectively. Ru lies at a six-fold coordinated position in the octahedron composed of six neighboring oxygens (four O_{Ru} and two O_{apical}) while Cu lies in a five-coordinated position (four O_{Cu} and one O_{apical}). The RuO_6 octahedra are rotated by about 14° around the c -axis, which leads to a significant modification in the electronic and magnetic structures; hence the magnetism of the Ru is sensitive to the structural distortion.⁵

The FLAPW calculations were performed based on the local spin density approximation, $L(S)DA$, with the Hedin-Lundquist exchange-correlation.^{13,14} Although the effects of electronic correlation in a strongly correlated system may be taken into account within a scheme such as $LDA+U$, $\text{RuSr}_2\text{GdCu}_2\text{O}_8$ shows metallic character even in the RuO_2 layers, which causes that effect to be weak and so may not alter our results. The intra-atomic noncollinear magnetism formalism^{14,15} was incorporated into the FLAPW method with no shape approximation for the magnetization density^{16,17}; in this, the density functional theory is treated with a density matrix with 2×2 components of the charge and magnetization density. Our approach allows the magnetic moment direction as well as the magnitude to vary continuously all over space, i.e., no shape approximation for the magnetization. The plane-wave was augmented with a spin-independent LAPW basis at the muffin-tin boundary. Although this approximation loses freedom compared with having a separate spin-up and spin-down LAPW basis, as is done in calculations for collinear magnetism, we confirmed that the accuracy was not degraded.¹⁸ The calculations were carried out without spin-orbit coupling (SOC), since the SOC induced energies,¹⁹ such as magneto-crystalline anisotropy energy that determines the easy direction, is expected to be much smaller than those of interest here.

The self-consistent calculations were started with an initial magnetization density depicted in Fig. 1(b), which

is a magnetic structure similar to a C-type AFM structure (Fig. 1(a)) but with the Ru moments slightly canted perpendicular to the AFM axis, i.e., to the FM axis direction in the figure. Here, the moment directions throughout the present paper are defined in a spin space since no SOC is taken into account. Although the neutron diffraction experiments⁶ revealed an AFM G-type ordering, we employed the C-type one in order to reduce the large computational effort this would entail. (The G-type ordering requires doubling the unit cell of the C-type ordering.) This is justified because the moment alignment along the c-axis is less important than that along the a-axis since the distance between the neighboring Ru atoms along the c-axis (11.56 Å) is significantly greater than that along the a-axis (3.84 Å).

The calculated spin magnetization density in the RuO₂ layer for the (110) and (001) planes is shown in Fig. 2 (a) and (b), respectively. The magnetism is clearly visible in the Ru, O_{Ru} and O_{apical} ions. The moments on the neighboring Ru sites order antiferromagnetically but their moments cant along the FM axis direction, which induces a ferromagnetic component of the magnetic moments. The canting of the Ru moments appears in the t_{2g} orbitals. The magnetization in O_{apical} is found to correlate with that in the Ru, where the O_{apical} $p_{x(y)}$ moments tilt in the same way as those in the Ru $d_{xz(yz)}$ orbitals. The O_{Ru} moments are also induced but point only along the FM axis direction, which correlates with the Ru d_{xy} states, as seen in Fig. 2(b). The Ru, O_{Ru} and O_{apical} magnetic moments inside the muffin-tin spheres are given in Table I, where the moments are projected along the AFM and FM axes. It is striking that the projected Ru moments along the AFM and FM axes result in magnetic moments of 1.16 and 0.99 μ_B , respectively, which have similar values to that observed by experiments, 1.18 μ_B when measured as the AFM structure by neutron diffraction⁶ and 1 μ_B as the FM value by magnetization.¹ However, a direct comparison of the projected FM moment with the experimental one would be difficult, since complicated behaviors, such as a spin-flop transition, accompany the high field experiments. Neutron diffraction⁶ demonstrated that the fields exceeding 0.4 T gradually enhance the FM intensity but decrease the AFM intensity; the highest field of 7 T results in a FM moment of 1.4 μ_B with no significant AFM intensity. In such a high field, the Ru moments tend to align in a collinear FM state, leading to the enhancement of the FM moments, which roughly agrees with the calculated moments ($\sim 1.5 \mu_B$) in the collinear FM state.⁵ Clearly, further investigations including the field dependence are necessary to fully describe the different experimental observations.

By introducing intra-atomic noncollinear magnetism, we found that the calculated total energy is only 10 meV/cell lower than that of the collinear AFM state. Thus, the canting of the Ru moments is energetically favored in the system. However, since the total energy difference is so small compared with T_m , there

would only be a short-range ferromagnetic ordering. This may be a reason why experiments, such as the neutron diffraction^{6,12} in the low-fields up to 0.4 T, could not clearly detect the ferromagnetic moments within their experimental sensitivity.

In order to discuss the Ru magnetism, we first consider the collinear AFM case and present the density of states (DOS) of the Ru t_{2g} in Fig. 3(a), where the x and z -axes are chosen as directions to the neighboring O_{Ru} and O_{apical} sites, respectively. The gray regions indicate the weight of the majority spin states. The magnetism of the Ru is dominated by antibonding t_{2g} states.⁵ The majority spin d_{xy} and $d_{xz(yz)}$ states on the Ru site can hybridize with the minority spin states on the neighboring Ru sites through O_{Ru} $p_{x(y)}$ and p_z orbitals by a superexchange mechanism. The majority spin d_{xy} and $d_{xz(yz)}$ states are almost fully occupied; therefore, the charge configuration of the Ru is close to t_{2g}^3 (Ru⁵⁺) with a high spin state, which prefers an antiferromagnetic alignment of their moments.²⁰ (Note that itinerant electrons are partially occupied in the minority spin Ru d_{xy} states, which creates an electron pocket at the Γ point in the Fermi surface, not shown, and leads to metallic RuO₂ layers.)

When the intra-atomic noncollinear magnetism is introduced, however, the admixture of the spin up and down states leads to an additional hybridization between the neighboring Ru ions, and results in the wider bandwidth of the t_{2g} states seen in Fig. 3(b). Although there is an admixture of the spin up and down states by introducing intra-atomic noncollinear magnetism, the spin-projected DOS along the average moment direction is plotted in the figure. The majority spin Ru $d_{xz(yz)}$ bands become more dispersive and cross the Fermi level (E_F) while the minority spin Ru d_{xy} bands are more occupied by itinerant electrons; this causes the system to be more metallic in character and close to a Ru⁴⁺ state with a low spin state configuration - as expected from experiments.^{7,21} Hence, a double exchange interaction due to the itinerant electrons that induces a weak ferromagnetism is promoted, and the magnitude of the Ru moments is significantly reduced from that expected from Hund's rule. Of course, the specification of the Ru valence states is, however, not exact due to the metallic character. It should be noted that this noncollinear magnetism arises from the band effects just discussed but does not have its origin in the SOC, such as via Dzyaloshinsky-Moriya interactions.²²

Finally, we comment the electronic structure of the CuO₂ bilayer. Even if the Ru moments cant, the Cu e_g band structure that is responsible to the high T_C superconductivity was found to be almost the same as those predicted by previous calculations of the collinear AFM state.⁵ This is because of an unique electronic structure of the layered Ru t_{2g} and Cu e_g states separated by O_{apical} p orbitals. The Ru t_{2g} states couple to the O_{apical} $p_{x(y)}$ orbitals which do not couple to the Cu e_g states.^{4,5} Therefore, as previously demonstrated,^{4,5} the strong hybridized Cu-O $dp\sigma$ orbitals, which show nest-

ing Fermi surface features similar to those in the high T_c cuprate superconductors, will give rise to anomalous behavior of the electronic properties arising from singularities in the generalized susceptibility. This is consistent with the possible coexistence of canted ferromagnetism and superconductivity in $\text{RuSr}_2\text{GdCu}_2\text{O}_8$.

In summary, first principles FLAPW calculations including intra-atomic noncollinear magnetism were performed to determine the magnetic structure of $\text{RuSr}_2\text{GdCu}_2\text{O}_8$. The magnetic moments on the neigh-

boring Ru sites order antiferromagnetically but cant perpendicular to the AFM axis. From the canting of the Ru moments, a double exchange interaction is exerted via itinerant t_{2g} electrons which can travel through the neighboring O p states. The results also suggest the possible coexistence of canted ferromagnetism and superconductivity in $\text{RuSr}_2\text{GdCu}_2\text{O}_8$.

Work at Northwestern University supported by the U. S. Department of Energy, Office of Science under Grant No.DE-FG02-88ER45372.

* Email address: kohji@phen.mie-u.ac.jp

¹ C. Bernhard, J. L. Tallon, Ch. Niedermayer, Th. Blasius, A. Golnik, E. Brücher, R. K. Kremer, D. R. Noakes, C. E. Stronach, and E. J. Ansaldo, Phys. Rev. B **59**, 14099 (1999).

² G. V. M. Williams and S. Krämer, Phys. Rev. B **62**, 4132 (2000).

³ Y. Tokunaga, H. Kotegawa, K. Ishida, Y. Kitaoka, H. Takagiwa, and J. Akimitsu, Phys. Rev. Lett. **86**, 5767 (2001).

⁴ W. E. Pickett, R. Weht, and A. B. Shick, Phys. Rev. Lett. **83**, 3713 (1999).

⁵ K. Nakamura, K. T. Park, A. J. Freeman, and J. D. Jorgensen, Phys. Rev. B **63**, 024507 (2001).

⁶ J. W. Lynn, B. Keimer, C. Ulrich, C. Bernhard, and J. L. Tallon, Phys. Rev. B **61**, 14964 (2000).

⁷ A. Butera, A. Fainstein, E. Winkler, and J. Tallon, Phys. Rev. B **63**, 054442 (2001).

⁸ A. Butera, A. Fainstein, E. Winkler, J. van Tol, S. B. Osleroff, and J. Tallon, J. Appl. Phys. **89**, 7666 (2001).

⁹ A. Fainstein, P. Etchegoin, H. J. Trodahl, and J. L. Tallon, Phys. Rev. B **61**, 15468 (2000).

¹⁰ J. D. Jorgensen, O. Chmaissem, H. Shaked, S. Short, P. W. Klamut, B. Dabrowski, and J. L. Tallon, Phys. Rev. B **63**, 054440 (2001).

¹¹ E. Wimmer, H. Krakauer, M. Weinert, and A. J. Freeman, Phys. Rev. B. **24**, 864 (1981); M. Weinert, E. Wimmer, and A. J. Freeman, Phys. Rev. B. **26**, 4571 (1982), and references therein.

¹² O. Chmaissem, J. D. Jorgensen, H. Shaked, P. Dollar, and J. L. Tallon, Phys. Rev. B **61**, 6401 (2000).

¹³ L. Hedin and B. I. Lundquist, J. Phys. C **4**, 2064 (1971).

¹⁴ U. von Barth and L. Hedin, J. Phys. C **5**, 1629 (1972).

¹⁵ J. Kübler, K. -H. Höck, J. Sticht, and A. R. Williams, J. Phys. F **18**, 469 (1988).

¹⁶ L. Nordström and D. J. Singh, Phys. Rev. Lett. **76**, 4420 (1996).

¹⁷ K. Nakamura, A. J. Freeman, Ding-sheng Wang, Lieping Zhong and Juan Fernandez-de-Castro, Phys. Rev. B **65**, 012402 (2001).

¹⁸ To confirm the accuracy, we performed FLAPW calculations using the spin-dependent and spin-independent LAPW basis for the collinear AFM C-type structure of $\text{RuSr}_2\text{GdCu}_2\text{O}_8$ (cf., Fig. 1 (a)) and found that both results are consistent. The calculated Ru and Gd magnetic moments showed the same values 1.57(-1.53) and 6.9 μ_B , respectively, in both cases.

¹⁹ R. Wu and A. J. Freeman, J. Magn. Magn. Mater. **200**, 498 (1999).

²⁰ J. Kanamori, J. Phys. Chem. Solids, **10**, 87 (1959).

²¹ R. S. Liu, L.-Y. Jang, H.-H. Hung, and J. L. Tallon, Phys. Rev. B **63**, 212507 (2001).

²² T. Moriya, Phys. Rev. **120**, 91 (1960).

Figures

FIG. 1: Schematic magnetic ordering of Ru and Gd moments in (a) collinear AFM and (b) noncollinear AFM structures of $\text{RuSr}_2\text{GdCu}_2\text{O}_8$, where the Cu, O_{Ru} , O_{Cu} and O_{apical} atoms are not given. The ordering of the Ru moments in (b) is similar to a C-type AFM ordering in (a) but the moments cant slightly out of their original direction, i.e., along the FM axis direction. Note that the moment directions are defined in a spin space since SOC is not taken into account.

FIG. 2: Spin magnetization density in the RuO_2 layer for the (110) and (001) planes of $\text{RuSr}_2\text{GdCu}_2\text{O}_8$, where the moment direction and magnitude are represented by arrow and the size, respectively.

FIG. 3: Density of states (DOS) of Ru t_{2g} states for (a) collinear AFM and (b) noncollinear AFM structures. The gray regions indicate the weight of their majority spin states.

Tables

TABLE I: Calculated magnetic moments, m (in μ_B), in the MT spheres of Ru, O_{Ru} and O_{apical} of $\text{RuSr}_2\text{GdCu}_2\text{O}_8$; here m_{AFM} and m_{FM} are projected moments along the AFM and FM axes in Fig. 1. Ru and O_{apical} have two sublattice sites.

| | m_{AFM} | m_{FM} | $ m $ |
|------------------------|------------------|-----------------|-------|
| Ru | ± 1.16 | 0.99 | 1.53 |
| O_{Ru} | 0.00 | 0.08 | 0.08 |

| | | | |
|---------------------|------------|------|------|
| O_{apical} | ± 0.08 | 0.07 | 0.11 |
|---------------------|------------|------|------|

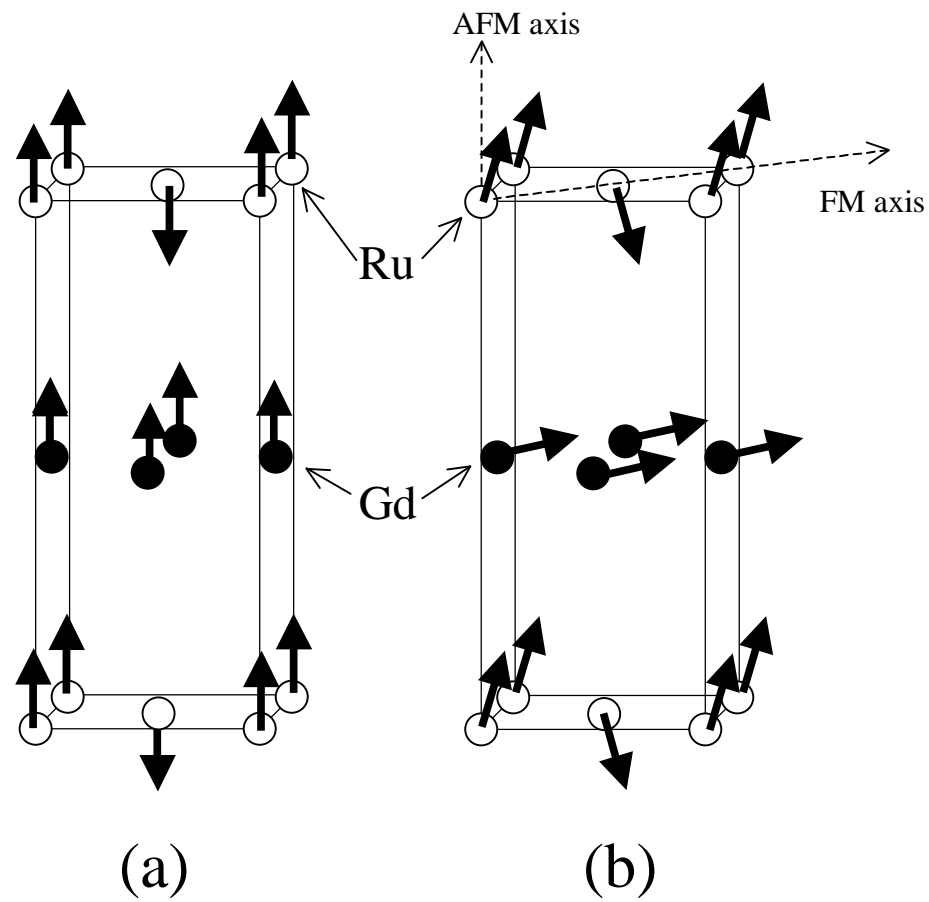


Fig.1 K. Nakamura et. al.

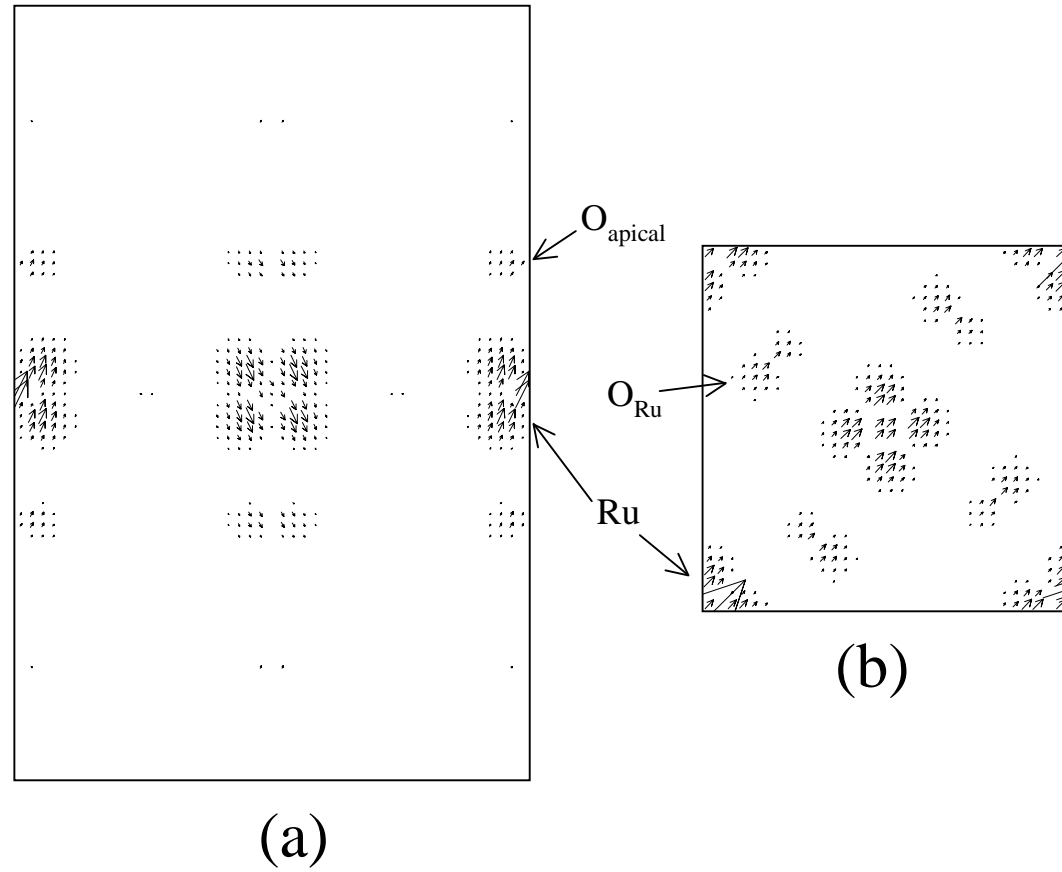


Fig.2 K. Nakamura et. al.

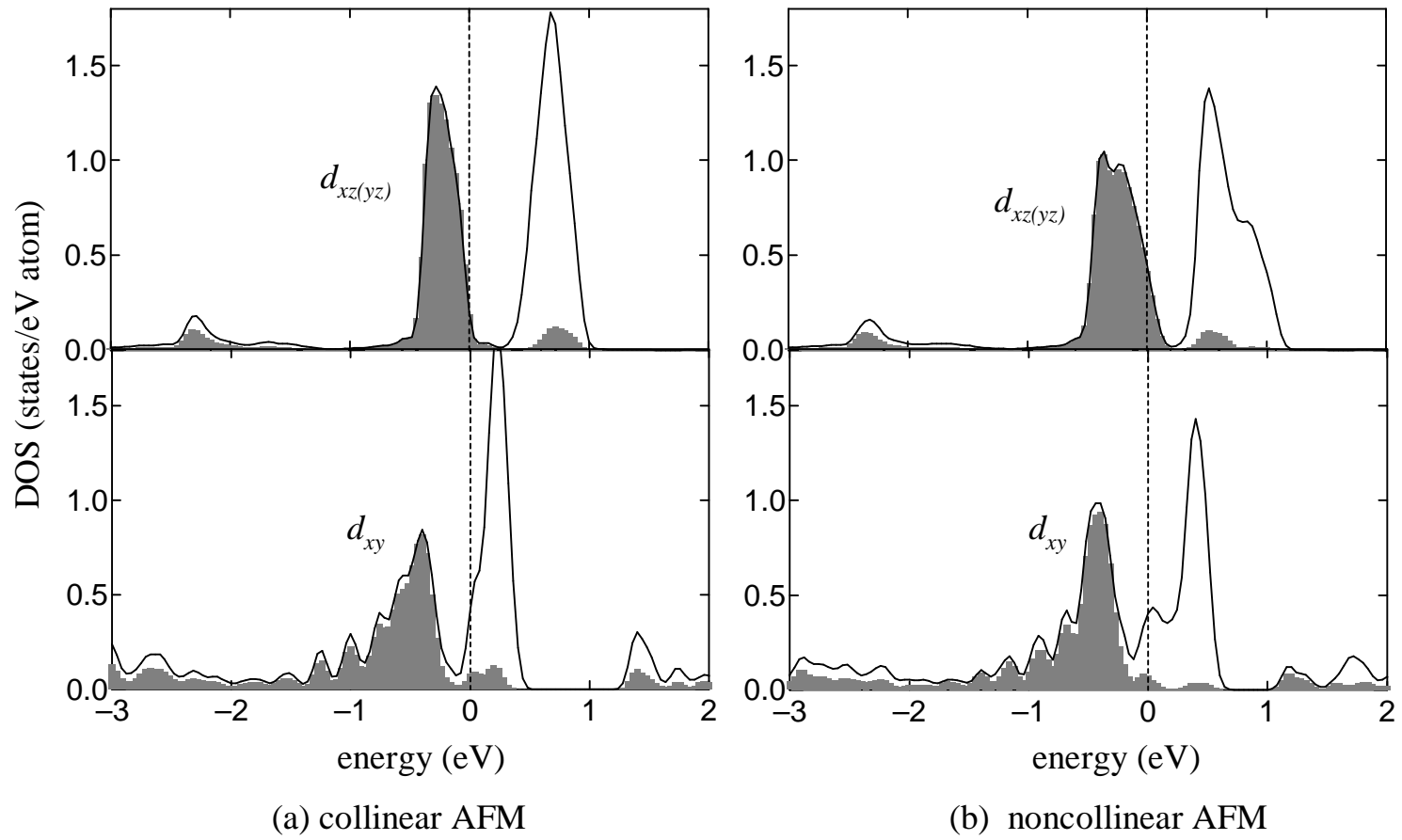


Fig.3 K. Nakamura et.al.